12th IEA Heat Pump Conference 2017

Full-scale experimental investigation of a heat-pump-based system for maximizing passive solar gains in housing–Preliminary results

Ian Beausoleil-Morrison[a,*], Sarah Brown[a], Sébastien Brideau[a]

[a]*Faculty of Engineering and Design, Carleton University, Ottawa, Canada*

Abstract

A full-scale experiment has been configured to explore a novel concept for capturing, extracting, and storing passive solar gains through windows by using radiant hydronic floors, a heat pump, and hot and cold thermal stores. More solar energy could be gained by increasing south-facing glazing areas, but this is typically avoided to prevent houses from overheating during certain times of the day and times of the year. The goal of the system examined here is to enable more south-facing glazing by converting the house into a low-grade solar collector whilst protecting against overheating. The preliminary results reported here show that the system can effectively collect and remove excess passive solar gains, and that the potential exists for storing and usefully exploiting this collected energy. Aspects of the design and system control requiring improvement have been identified.

Keywords: Passive solar heating, house, heat pump, hydronic floors

1. Introduction

1.1. Motivation

Passive solar gains through windows can significantly reduce space heating requirements. However, the amount of south-facing glazing is often restricted to modest levels in low-energy houses to protect against overheating during times of high solar gain, thus preventing the full exploitation of the solar energy resource. Moreover, there is a temporal mismatch between passive solar gains (daytime, centred around solar noon) and peak heating loads (night).

We are studying a novel concept to increase the contribution of solar energy for meeting space heating and domestic hot water heating demands. This involves using a large area of south-facing windows to increase passive solar gains, combined with an active system composed of radiant hydronic flooring, a heat

*Corresponding author, Ian_Beausoleil-Morrison@carleton.ca

pump, hot and cold thermal stores, and circulation pumps. This concept is illustrated schematically in Figure 1. Cool water is circulated from the cold thermal store through the radiant floors to prevent overheating during times of high passive solar gains. The heat pump is used to transfer energy from the cold thermal store to the hot thermal store, which can then serve domestic hot water needs, or can be used to provide space heating through the radiant floors during periods of heating demand. In this way, the active system essentially converts the house into a low-grade solar collector whilst protecting against overheating.

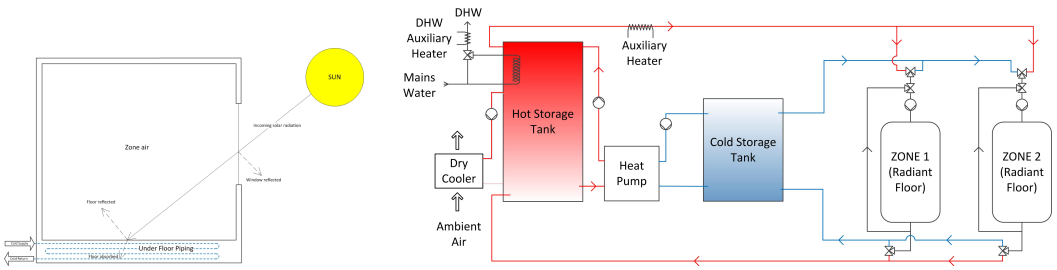

(a) Capturing excess passive solar gains with radiant floor

(b) Heat-pump-based active system

Fig. 1: Concept for enabling increased passive solar gains

1.2. Literature review

Passive measures such as orienting windows to the south to capture solar gains during the heating season are commonly used to lower house heating demands. However, not all passive solar gains can usefully offset space heating demands, as they may be received when the house does not require heating and could therefore lead to overheating. Although building elements that absorb the incoming solar radiation can store the energy for later release to the indoor air space, such passive storage methods have little benefit in many situations. Sander and Barakat [1] showed that with well insulated and airtight houses, the addition of thermal mass has minimal impact on reducing space heating demand in the Canadian climate. They also showed that the optimal south-facing glazing area for reducing heating demand is approximately 4.8% of floor area when triple-glazed windows are used, and 3.4% for double-glazing.

More recently Proskiw [2] examined the potential benefits of heavy concrete construction versus light-weight wood-frame construction for Canadian houses. They found this costly change might yield a 2-7% reduction in heating demand, reinforcing the earlier findings of Sander and Barakat [1]. Proskiw [2] also recommended a maximum south-facing glazing area of 6% of floor surface area, finding that more window area would have minimal benefits in reducing heating demands due to overheating during certain times of the day and times of the year.

Radiant hydronic floors can be used to heat and cool buildings. Olesen [3] reports that in the absence of solar gains, a maximum cooling rate of 42 W/m^2 can be achieved with floor cooling for typical conditions. If however solar gains are incident on the floor, the cooling capacity of the floor increases. For example, Simmonds et al. [4] designed and modelled the mechanical system of an atrium at the Bangkok airport whose building envelope incorporated glazing with a low solar transmissivity. They found that the floor cooling capacity was approximately 80 W/m^2 when solar gains were incident on the floor. Olesen [3] reports a simulated case study of an atrium with displacement ventilation and radiant floors in which the cooling capacity was found to be as high as 150 W/m^2. Although the radiant floors were found to have little influence on the zone air temperature, the operative temperature was reduced significantly.

The studies cited here have shown that south-facing glazing areas are commonly limited to prevent overheating, thus sacrificing the potential of exploiting greater solar gains through windows. They have also shown the potential for using radiant hydronic floors to cool spaces in which solar radiant gains are absorbed by the floor. However, no reports could be found in the literature that examine the concept outlined in the previous subsection of using radiant hydronic floors to protect houses against overheating caused by

excessive passive solar gains while capturing, storing, and using this otherwise foregone renewable energy resource.

1.3. Previous work

In previous work we have studied the potential energy savings that could be realized by substantially increasing south-facing glazing area in Canadian housing and incorporating the active heat-pump-based system. A detailed set of building performance simulations was conducted and reported in Brideau et al. [5]. A single-family detached wood-framed house situated in Ottawa, Canada was the object of the study. The performance of the system described in Section 1.1 and illustrated in Figure 1 was predicted for a highly-glazed house; the south-facing-glazing to floor-area ratio was 14.4%, more than double that recommended by Sander and Barakat [1] and Proskiw [2]. This scenario was compared to a reference case that had more typical glazing area and a conventional HVAC system.

The analysis indicated that energy savings up to 24% might be achievable. It also found performance to be sensitive to storage volumes. These findings must be treated as preliminary, however, due to the significant number of modelling uncertainties related to:

- Predicting the distribution of solar irradiance to internal building surfaces.
- Convective heat transfer between floor internal surfaces and the room air.
- Heat transfer between the floor surfaces and the hydronic pipes.
- Ground-reflected solar irradiance.
- Transient behaviour of the heat pump.
- Stratification within the water stores.

New models have been developed and validated to reduce some of this modelling uncertainty. Brideau and Beausoleil-Morrison [6] report on the development of an above-floor tube-and-plate (AFTP) radiant hydronic floor model. This consists of a 2D transient finite difference model coupled to the analytic tube model of Laouadi [7], which is then coupled to 1D conduction models in building performance simulation tools. This model has been verified using a transient 2D finite-element code and validated using empirical data gathered from full-scale experiments [8].

A transient residential-scale water-water heat pump model has also been developed [9]. This involves a performance map coupled with time constants to estimate performance during startup. These time constants vary depending on the elapsed time since the heat pump was last switched from energized to de-energized state. This approach was found to give better predictions of the heat transfer rates at the condenser and evaporator than could be achieved with a steady-state modelling approach.

1.4. Objectives and outline of paper

This paper describes the next phase in our exploration of this unproven concept aimed at increasing the contribution of solar energy for meeting space heating and water heating demands. In it we describe the full-scale experiment we have configured and report our preliminary findings. The research house, including the design of the radiant floor and hydronic systems, is described in the next section. Following this, the instrumentation used to measure performance during the experiments is described and measurement uncertainties treated. The results from an experiment aimed at examining the radiant hydronic floor's ability to capture solar gains and cool the house are then examined. The first experiment conducted with the complete system is then described and detailed results are examined to give a preliminary assessment of the concept. Conclusions are then drawn and recommendations made for future work.

2. Experimental configuration

2.1. Research house

A full-scale experimental facility has recently been designed, constructed, and commissioned for conducting long-term explorations of novel and unproven concepts aimed at radically reducing the reliance

Fig. 2: The Urbandale Centre for Home Energy Research viewed from the southwest

of Canadian housing on conventional energy sources. Located on the Carleton University campus in Ottawa, this research house, known as the *Urbandale Centre for Home Energy Research* (see Figure 2), has a footprint of 6.1 by 12.2 m and includes a full-height basement and two above-grade stories.

The house is of wood-frame construction and contains more insulation than required by current regulations, but intentionally is not insulated more heavily than would be viable with current construction practices. The above-grade south-, east-, and west-facing walls have a nominal U-value of 0.21 W/m^2K; the north-facing wall has a nominal U-value of 0.12 W/m^2K; and the attic insulation has a nominal U-value of 0.11 W/m^2K. The insulation under the basement floor and around the structural footings has a nominal U-value of 0.36 W/m^2K while the insulation added to the basement walls has a nominal U-value of 0.21 W/m^2K. The building's airtightness at 50 Pa depressurization was measured to be 1.3 ac/h.

All windows are triple-glazed with two low-emissivity coatings and argon gas fill. The windows have a nominal centre-of-glass U-value of 0.79 W/m^2K and a SHGC (g-value) of 0.62. Most of the house's windows are placed on the south façade. The east and west façade include a modest amount of window area, whereas no windows face north. The total south-facing glazed area is 20 m^2 which greatly exceeds the recommended levels discussed in Section 1.2. The east- and west-facing glazed areas are 2.6 and 2.5 m^2, respectively.

The research house possesses redundant energy conversion, storage, and distribution systems to enable research on numerous topics with minimal switch-over time required. There is a large array of evacuated-tube solar-thermal collectors (seen in Figure 2), two buried seasonal-thermal stores, an air-source heat pump coupled to a rock-bed thermal store, a water/water heat pump, radiant hydronic floors, supply and return ducts, an energy-recovery ventilator connected to dedicated ducting, and an auxiliary electric boiler.

The two above-grade storeys are configured with low-mass AFTP radiant hydronic floors that consist of subflooring, EPS insulation, aluminum fins, and PEX piping. These are finished with thin concrete backing boards and ceramic tiles, with thin layers or mortar. A cross-sectional schematic of the floors is shown in Figure 3 along with a photograph taken during construction.

The research house includes a complex hydronic network to facilitate easy switching between energy systems. This is shown schematically in Figure 4. The components illustrated in the system concept of Figure 1b can be found in this schematic. The cold storage tank can be seen in the bottom left of Figure 4 and the heat pump can be seen in the top right. The hot storage is actually realized with three segmented tanks, this to allow exploration of storage volume upon system performance: these are the *RE 119 D1* and *RE 119 D2* tanks seen in the centre of the schematic, and the *Turbomax* tank at the centre right.

The water/water heat pump used in the current research has a nominal cooling capacity of 11 kW and employs R134a as its refrigerant. Because the house is unoccupied, a DHW mimicry system was configured to draw quantities of water at programmed intervals from the *Turbomax* hot storage tank. The tanks and controlled valves making up this system can be seen at the bottom centre of Figure 4.

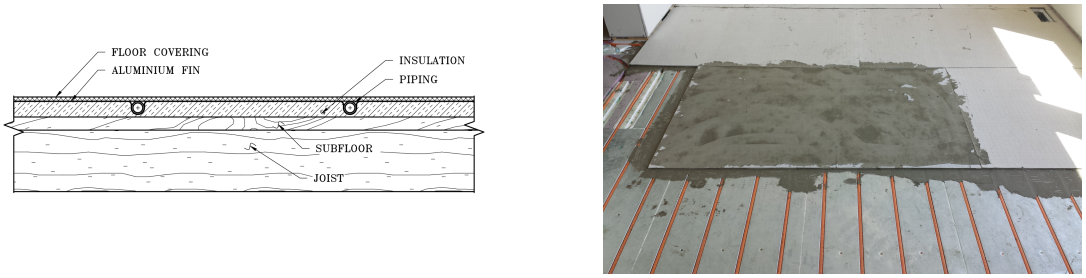

(a) Cross-sectional schematic

(b) Insulation layer, aluminum fin, hydronic tubes, mortar, and concrete board

Fig. 3: Hydronic flooring in research house

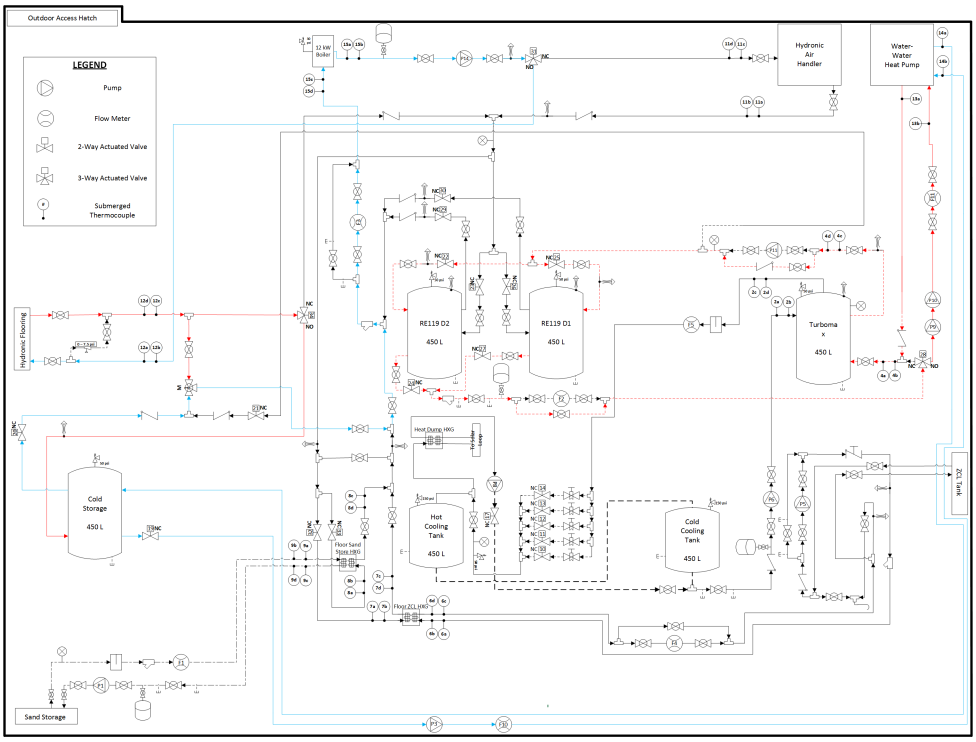

Fig. 4: Hydronic network and instrumentation placement

2.2. *Instrumentation, calibration, and measurement uncertainty*

The research house is heavily instrumented to measure its thermal conditions and energy flows relevant to assessing system-level and component-level performance. A central data acquisition and control (DAQ) system is used to log sensor readings as well as to control the valves and pumps illustrated in Figure 4.

Pyranometers are mounted on the roof and the exterior surface of the south façade. Secondary reference pyranometers are used to measure the global horizontal irradiance and the total irradiance on the exterior surfaces of the windows with a high-degree of accuracy, whereas the diffuse horizontal irradiance is determined with a pyranometer with multiple sensors and shading bands. Ambient air temperature, relative humidity, wind speed, and wind direction sensors are also mounted on the roof.

The solar irradiance transmitted through the south-facing windows is directly measured using a vertically oriented secondary reference pyranometer. The indoor air temperature is sensed using copper-constantan (Type T) thermocouples that are mounted within aspirated radiation shields. Currently 18 such sensors are used to measure the air temperature at various locations and elevations within the house.

Thermocouples and multi-junction thermopiles were fabricated and immersed within fluid streams throughout the hydronic network illustrated in Figure 4. This was accomplished by inserting the wires through machined holes in specially fabricated compression fittings and then soldering the beads in place. Immersing these beads in the flow streams provides highly accurate and fast-responding sensing. All such sensor locations are indicated in Figure 4. Refer, for example, to the loop supplying hot or cold water to the *hydronic flooring* loops at the centre left of the figure: *12a* and *12b* are thermocouples that sense the temperature of the water supplied to the floors, whereas *12c* and *12d* are thermocouples that sense the temperature of the water returned from the floors. (Duplicate thermocouples are used for data checking and redundancy reasons.) Additionally, a 6-junction thermopile is located at this position to accurately measure the difference in temperature between the supply and return streams.

The thermopiles and thermocouples were calibrated using two precision-controlled water baths and two Pt100 platinum resistance thermometers. The cold junctions of the thermopile were immersed in one bath along with one of the Pt100 thermometers, while the hot junctions and the other Pt100 thermometer were immersed in the other bath. The bath temperatures were then controlled to span the full range of expected temperatures. The thermopile's voltage signal was then calibrated to the Pt100 temperature measurements from this calibration data set using a regression equation.

All possible sources of bias errors were accounted for during this calibration procedure and during the experiments. This included the DAQ's resolution for reading voltages, the bias error of the Pt100 thermometers, imperfections in the calibration regression, temperature fluctuations in the laboratory during the calibration process, and the thermistors used to measure the temperature of the cold junction at the DAQ. When all of these individual sources of bias error were combined using the root-sum-square method recommended by Moffat [10], it was found that temperatures could be determined with the thermocouples with a total bias error of ± 0.5°C and that temperature differences could be determined with the thermopiles with a total bias error of ± 0.1°C.

Positive displacement flow meters of the oval-gear type are used to measure fluid flow rates. These devices produce a pulse signal whose frequency is proportional to volumetric flow rate. For example, *F10* located at the bottom centre of Figure 4 measures the water flow rate between the cold tank, pump *P3*, and the heat pump's evaporator. Each flow meter was calibrated by the manufacturer and certified to have a bias error ±1% of the reading.

The primary measurements taken by the above mentioned instruments were used to derive a number of quantities of interest in assessing performance of the system. For example, the rate of heat transfer from the radiant floors to the water stream supplied by the cold tank via pump *P14* was derived from thermopile and flow meter measurements. This was accomplished by treating the water as an incompressible fluid with constant density and specific heat with the following equation,

$$q_{floor} = \left(\rho \cdot \dot{V} \cdot c_P \cdot \Delta T\right)_{floor} \tag{1}$$

where $\dot{V}$ is the volumetric flow rate of water circulated through the radiant floors measured with flow meter *F3* and ΔT is the temperature increase of the water from the floor's inlet to its return measured with the thermopile at location 12. ρ and c_P are the density and specific heat of the water, respectively. These are treated as constant and evaluated at 15°C, the approximate average temperature of the water throughout the experiment.

The bias errors associated with the measurement of $\dot{V}$ and ΔT propagate uncertainty into the derivation of q_{floor}. When this, as well as the uncertainty associated with approximating ρ and c_P as constant, were considered, it was found that q_{floor} could be determined within ±2% using the methods recommended by Moffat [10] to propagate measurement uncertainties into derived quantities.

Similar methods were used to determine the bias errors of the other derived quantities reported in this paper. Data were sampled at a 1-second or 10-second frequency and then averaged to either 10-second

intervals or 5-minute intervals. But in the graphs that follow the data are typically plotted at a 5-minute frequency to improve the clarity of presentation.

3. Capture of passive solar gains by floor

An experiment was conducted with the active cooling system to ascertain its ability to cool the house while it was receiving solar irradiance. This experiment was conducted for a midday period slightly longer than three hours, and was preceded by an overnight period during which the house free floated. Although the outdoor air temperature dropped to 13°C overnight, the indoor air temperature remained around 24°C due to the solar gains that had been absorbed by the house the previous day. All windows remained closed during the experiment, eliminating any possibility of ventilative cooling.

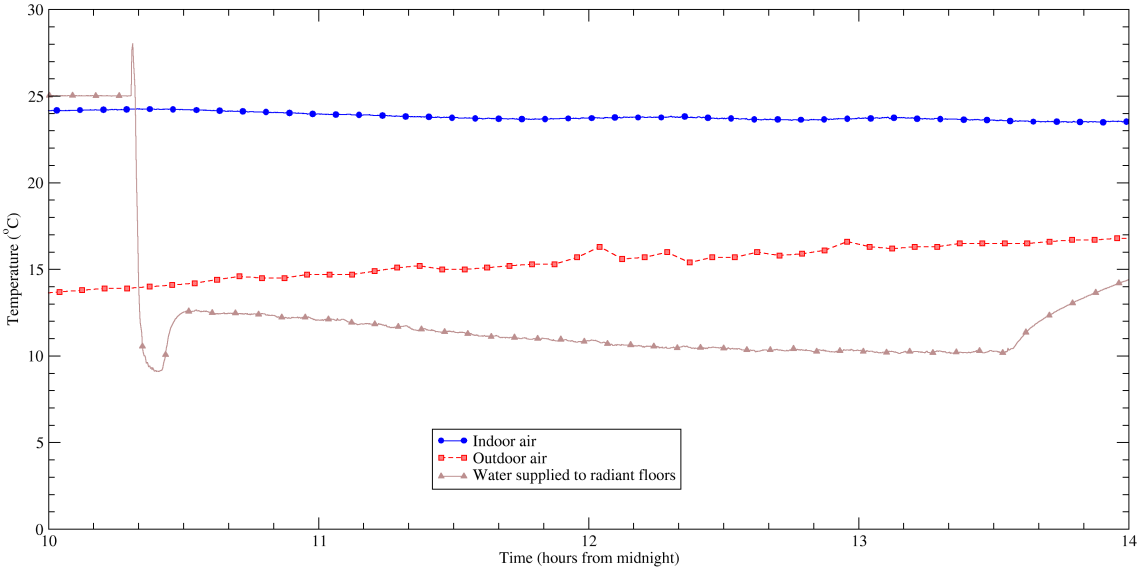

Fig. 5: Temperatures during experiment to assess floor's ability to capture solar gains

The experiment commenced at 10h18 when the pump (*P14* in Figure 4) was cycled on to circulate water from the cold tank to the radiant floors. This pump continued to operate for more than three hours, until 13h31. As can be seen in Figure 5, when the pump cycles on there was a sudden change in the readings from the thermocouples immersed in the pipe that supplies the radiant floors (*12a* and *12b* in Figure 4). Initially the temperature rose by 3°C as warm water that had stagnated in the pipes was pushed through the pipes to the floor. But then, after about a minute, cold water from the tank reached the thermocouple location. Due to the continuous operation of the pump during the experiment, the temperature sensed by these thermocouples provided a good representation of the cold tank's temperature.

As can be seen in Figure 5, the temperature of the cold tank was initially less than 10°C, but it rose to almost 13°C after 10 minutes. This warming was caused by the hot water returning from the radiant floors to the tank, and also likely due a disruption of the tank's stratification by the inlet and outlet flows.

The heat pump was cycled on 4 minutes after the floor pump and it ran continuously until 4 minutes before the end of the experiment. During this time the heat pump continuously extracted energy from the cold tank, transferring it to the hot tanks. In this way, the temperature of the cold water supplied to the floors remained between 9 and 13°C throughout the entire 3 hour experiment.

Readings from the 18 thermcouples mounted in aspirated radiation shields were averaged to determine the house's mean indoor air temperature. These temperatures are also plotted in Figure 5. As can be seen from the figure, the house was gradually cooled by the radiant floors during this 3-hour experiment. The

mean indoor air temperature was approximately 0.7°C cooler at the end of the experiment than it was at the start.

Figure 6 illustrates how q_{floor} varied over the course of the experiment. As can be seen, q_{floor} rose to almost 20 kW immediately after the circulation pump was cycled on, and then dropped quickly to 8 kW (73 W/m^2) within 10 minutes. The initial spike in q_{floor} was caused by the volume of water that lay stagnant in the radiant floor's hydronic loops (~120 L). During these initial few minutes, the water returning from the radiant floors was quite hot relative to the supply water temperature until this stagnant water had been flushed out. But after the initial 10 minutes, the water returned from the floors at a cooler temperature, resulting in a lower value of q_{floor}. It can also be seen from Figure 6 that q_{floor} decreases gradually throughout the experiment to a final value of about 5.5 kW (50 W/m^2). These rates of heat flux are within the range of values reported in the literature that was reviewed in Section 1.2.

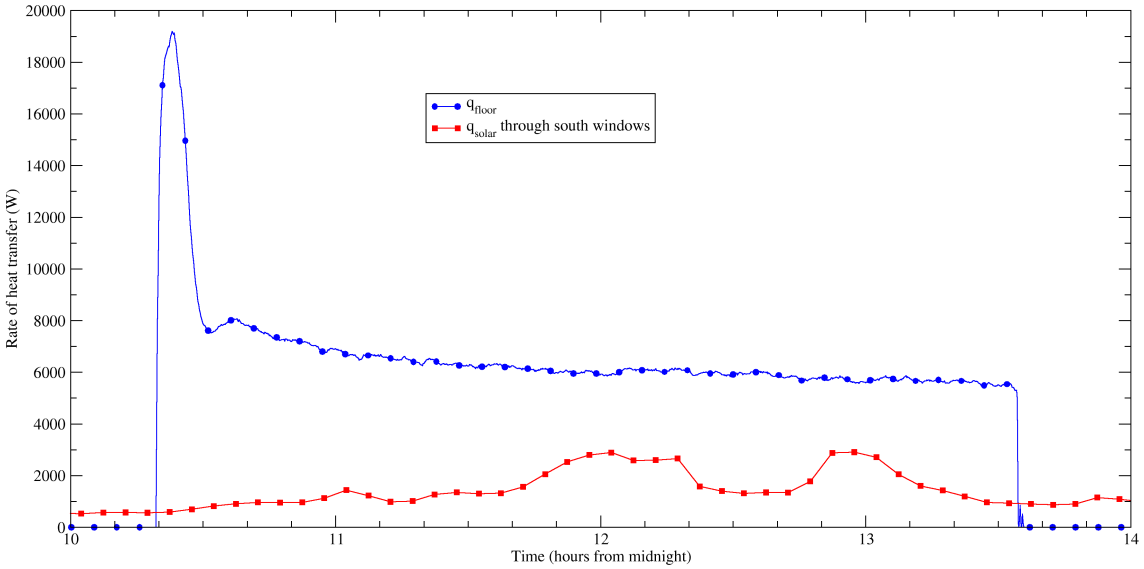

Fig. 6: Heat transfer during experiment to assess floor's ability to capture solar gains

Conditions on the day of this experiment were mostly overcast with some sunny periods. The pyranometer mounted vertically inside the house continuously measured the solar irradiance that was transmitted through the south-facing windows. The product of these measurements and the glazed area of the windows provides an estimate of the solar radiation entering the house through its south windows. This quantity is also plotted in Figure 6. As can be seen, the solar radiation reached as high as 3 kW during sunny periods around 12h and 13h. Although difficult to see due to the scale of Figure 5, these increases in solar gains caused some short-term heating of the indoor air. Notwithstanding, it can be seen from Figures 5 and 6 that the active system was able to not only extract the solar gains over the course of the experiment, but also to cool the house at a modest rate.

4. Complete system testing

An experiment spanning over a three-day period was then conducted to assess the functioning of the complete system. The data gathered during October 12 are examined in this section. The weather conditions during this day can be seen in Figure 7. The goal had been to conduct this experiment during a cool autumn day during which the house would experience cooling demands during the day and heating demands during the night. However, as can be seen the outdoor air temperature dropped to only 8°C by early morning

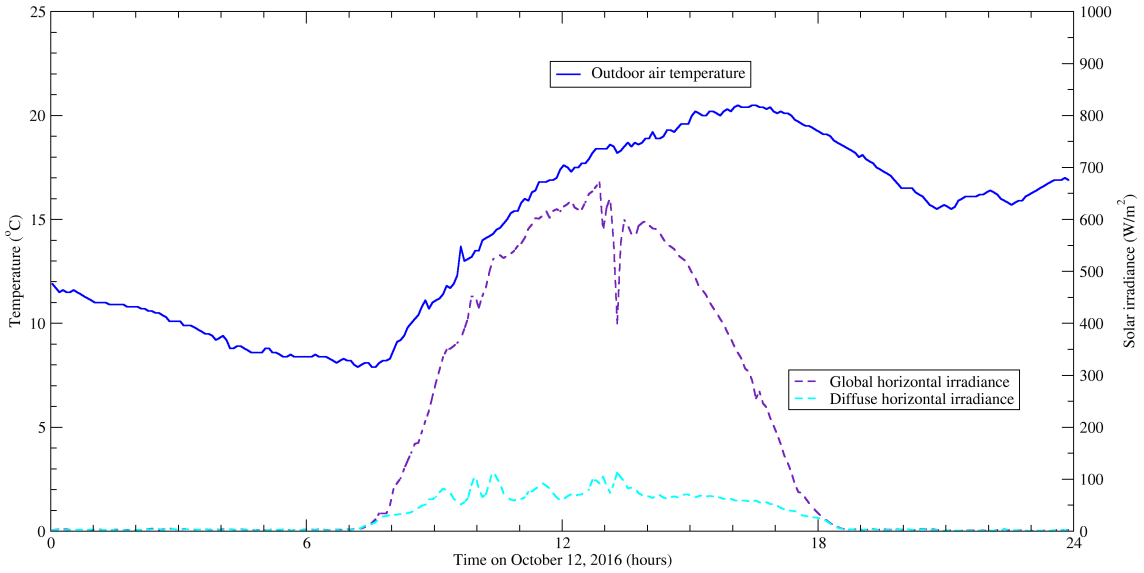

Fig. 7: Weather during complete system experiment

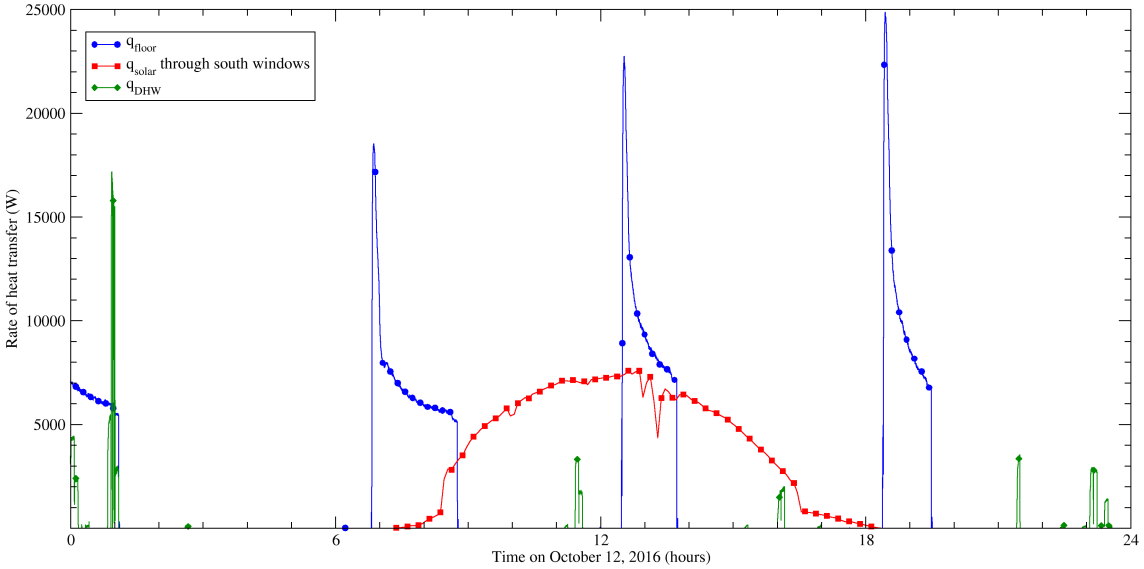

Fig. 8: Energy transfer rates during complete system experiment

and rose to 21°C by late afternoon. Furthermore, the sky was nearly cloudless, as evidenced by the global horizontal and diffuse horizontal irradiance measurements shown in the figure.

The cloudless conditions combined with the low sun elevation of October resulted in significant solar gains to the house, as can be seen in Figure 8. The red line shows that the solar gains through the south facing windows peaked at nearly 8 kW just after noon. It is worth noting that this rate of heat addition exceeds the house's peak heating load that is required when the outdoor air temperature is -30°C and when there are no solar or internal heat gains.

Figure 8 also illustrates the rate of heat transfer from the radiant floors to the water stream over the

course of the day (blue line). Each time the pump that circulates cold water to the radiant floors cycled on, there was a spike in the rate of heat transfer for the reasons explained in Section 3. This can be seen around 6h45, 12h30, and 18h20. Following this, the rate of heat transfer from the radiant floors diminished to between 5.5 and 10 kW until the pump cycled off again.

The reasons for the cycling of the floor pump are revealed in Figure 9. This figure plots the temperatures of the indoor air (purple), the hot tanks (red), and the cold tank (blue), as well as the flow rate of water to the radiant floors (green). This shows that, for example, the pump stopped circulating cool water to the radiant floors at 1h05 despite the fact that the house's air temperature had not yet cooled to its setpoint of 25°C. In fact, it was the temperature of the hot tanks that triggered this action, it having risen to 60°C. This initiated a *heat dump* operation to protect the heat pump, which could not operate with condenser inlet temperatures above 62°C. During the heat dump, water was circulated between the hot tanks and an external heat sink (a buried heat store next to the building) to cool the tank. Due to the configuration of the hydronic system (refer to Figure 4), the heat pump could not continue to operate during this heat dumping operation. As several hours were required to reduce the temperature of the hot tanks to 42°C, this operation essentially prevented the active system from cooling the house.

Once the hot tanks had been sufficiently cooled and the heat dump operation suspended, the heat pump was finally able to cycle back on at 6h15 and it was able to rapidly cool the cold tank. Once the cold tank temperature dropped to 9°C, the pump (*P14* in Figure 4) once again began circulating cold water to the radiant floors. As can be seen in Figures 8 and 9, this pump operated continuously from 6h50 to 8h45 and heat was extracted from the radiant floors and transferred to the cold tank. For most of this period the rate of heat extraction by the radiant floors was between 5.5 and 8 kW, and the indoor air was cooled from 26 to 25°C. Unfortunately, this pump was forced to cycle off at 8h45 because the hot tanks had once again been heated to 60°C and another heat dump operation was required. As a consequence of suspending the cooling operation the air temperature in the house rose quite rapidly in response to the solar gains (refer to Figure 7).

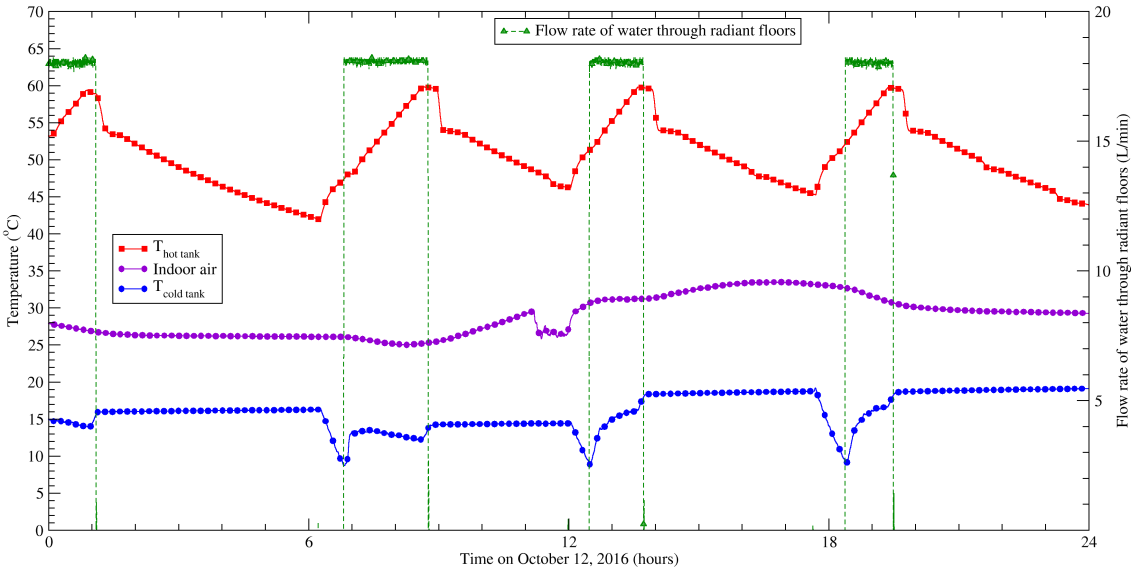

Fig. 9: Indoor air and hot and cold tank temperatures during complete system experiment

The heat pump's operation is illustrated in Figure 10, which plots the electric power draw and the rates of heat transfer at the evaporator and condenser over the course of the day. The morning operational sequence of the heat pump discussed in the previous paragraph can be clearly seen in this figure. The heat pump was switched on at 6h15 after the heat dump from the hot tanks was completed and it operated continuously for

40 minutes to cool the cold tank to its setpoint of 9°C. The heat pump then cycled off, but because the pump circulating cold water to the radiant floors had cycled on just 5 minutes earlier, the cold tank's temperature began rising, and this triggered the heat pump to cycle back on 5 minutes later (the 5-minute delay was forced by the heat pump's internal controls). The heat pump then ran continuously for the next 95 minutes until just before the next heat dump sequence.

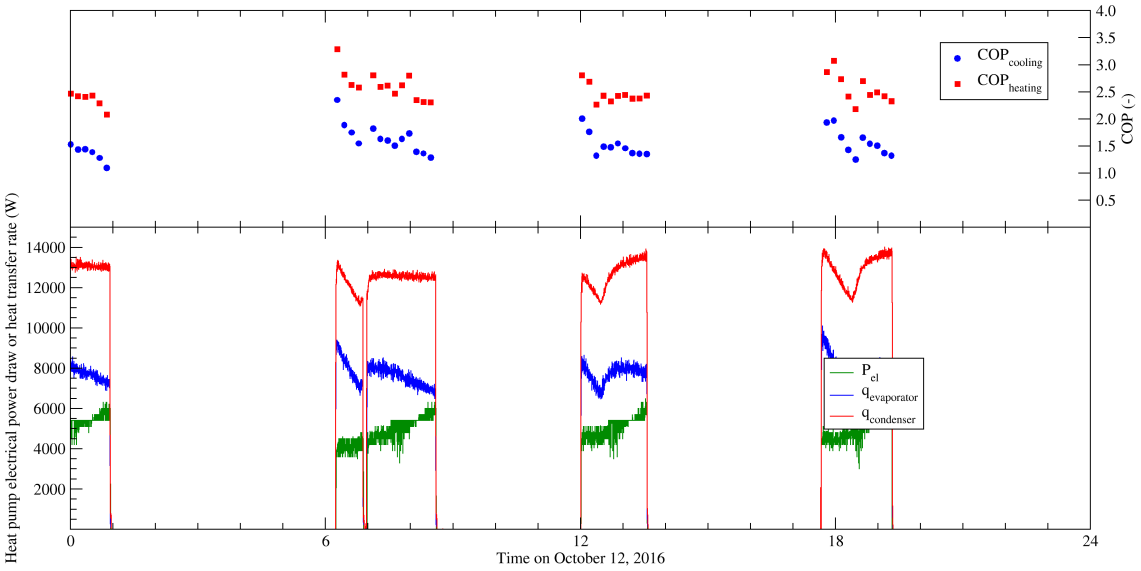

Fig. 10: Heat pump operation during complete system experiment

During this sequence from 6h15 to to 8h35, it can be seen from Figure 10 that the heat pump was extracting energy from the cold tank at the rate of about 8 kW while the radiant floors added energy to the tank at the rate of 5.5 to 8 kW (see Figure 8). Over this time period the heat pump extracted 62 MJ of energy from the tank, whereas the radiant floors added 47 MJ. The difference between these numbers is accounted for by energy storage within the tank (the temperature was about 5°C colder at the end of the cycle than at the beginning), and to a much lesser extent due to heat transfer between the room and the tank and between the room and the pipes.

Figure 10 shows how the electrical power draw of the heat pump increased between 6h15 to to 8h35, this due to the rising temperature of the hot tanks and the decreasing temperature of the cold tank. This trend is also seen in the top of the figure, which plots the heating and cooling COPs over the day. Over each operational cycle, the cooling COP decreases from about 2 to about 1.25, while the heating COP decreases from around 3 to just over 2.

Some of the energy added to the hot water tank by the heat pump was used to meet domestic hot water (DHW) needs. The quantity and timing of hot water draws from the tank applied in this experiment are shown in Figure 8.

The active system was unable to maintain comfort conditions within the house, as clearly illustrated in Figure 9. (Note that the sudden and temporary reduction of the indoor air temperature between 11h00 and 12h00 was caused by the opening of a window during one of the heat dump operations.) The main reason was the interruption in cooling due to the heat dump operation. Notwithstanding, the radiant floor system was able to extract much of the solar gains occurring over the course of the day. A total of 165 MJ of solar gains were transmitted through the south-facing windows (the integration of the red line in Figure 8). Due to the heat dumping, the radiant floors were only able to operate for about 4.5 hours, but during this time they managed to extract 162 MJ of energy from house, a value almost equal to the solar gains. The heat pump consumed 116 MJ of electricity and added 294 MJ of energy to the hot tanks. As the DHW draws during this

experiment were very low, only 13 MJ were extracted from the hot tanks to supply these needs, and much of the remaining energy had to be dumped to protect the hot tanks from overheating. Had more representative DHW demands been used, or had this experiment been run on a colder day, much of the energy from the hot tanks could have been used to supply DHW or space heating at night rather than being dumped.

5. Conclusions

This paper has presented the first results from the full-scale experimental investigation of a novel concept aimed at increasing the contribution of solar energy for meeting space heating and water heating demands. The heat-pump-based active system that is used to capture and store excessive passive solar gains using radiant hydronic floors was described. Our experimental configuration was detailed, as were the measurement methods we employ to assess performance. The results from our first two experiments with the system were then presented.

The first experiment was aimed at assessing the system's ability to cool the house while it was receiving solar irradiance and was conducted for a midday period on October 1 for slightly longer than three hours. During most of this experiment cold water was continuously circulated to the radiant floors and the heat pump ran continuously to transfer energy from the cold storage to the hot storage. After an initial spike, it was found that the radiant floors transferred heat to the circulating water stream at a rate of 8 kW (73 W/m^2) and then gradually decreased to a rate of 5.5 kW (50 W/m^2) by the end of the experiment. These rates of heat transfer were found to be consistent with values reported in the literature for cooling spaces with radiant floors. The mean indoor air temperature dropped by 0.7°C over this experiment. It is suspected that this slow rate of decline in the indoor air temperature is because the floors are cooling the building structure radiatively and that there is considerable lag associated with these surfaces convectively cooling the indoor air. This will be explored in future experimentation.

The second experiment explored the functioning of the complete system, including providing DHW loads from the captured solar energy. A complete day's worth of data were examined for a warm and cloudless October day. Many challenges for designing and operating this system were revealed during this experiment. For example, the hot tanks could not store all of the solar energy that was gathered by the radiant floors and upgraded by the heat pump. As a result, a significant amount of energy had to be rejected from the hot tanks during the experiment. Unfortunately, due to the design of the hydronic system in the research house this heat dumping operation could not be run concurrently with the heat pump. Consequently, the radiant floor cooling processes was interrupted on several occasions, which resulted in overheating of the building. In future work we will reconfigure the hydronic system to avoid this problem. As well, experiments will be conducted with more realistic DHW demands and on colder days–and for longer time sequences–so that the captured solar energy can be stored and utilized to provide space heating at night. Notwithstanding these problems, the active system was able to extract almost the entirety of the solar gains that were transmitted through the house's large area of south-facing glazing over the day.

References

[1] D. Sander, S. Barakat, Mass & Glass: How Much? How Little, ASHRAE Journal 26 (11) (1984) 26–31.
[2] G. Proskiw, Identifying affordable net zero energy housing solutions, Tech. Rep., Natural Resources Canada, 2010.
[3] B. Olesen, Possibilities and Limitations of Radiant Floor Cooling, ASHRAE Transactions 103 (1) (1997) 42–48.
[4] P. Simmonds, W. Gaw, S. Holst, S. Reuss, Using radiant cooled floors to condition large spaces and maintain comfort conditions, ASHRAE Transactions 112 (1) (2000) 695–701.
[5] S. Brideau, I. Beausoleil-Morrison, M. Kummert, Collection and storage of solar gains incident on the floor in a house during the heating season, Energy Procedia 78 (2015) 2274–2279, ISSN 1876-6102, doi:10.1016/j.egypro.2015.11.364.
[6] S. Brideau, I. Beausoleil-Morrison, Model Development for Tube-in-Subfloor Radiant Floor Heating and Cooling, in: Proc. eSim 2014, Ottawa, Canada, 853–866, 2014.
[7] A. Laouadi, Development of a radiant heating and cooling model, Building and Environment 39 (4) (2004) 421–431.
[8] S. Brideau, Collection and storage of solar gains incident on a radiant floor in highly glazed houses, Ph.D. thesis, Carleton University, 2016.
[9] S. Brideau, I. Beausoleil-Morrison, M. Kummert, Empirical model of a 11 kW (nominal cooling) R134a water-water heat pump, in: Proc. eSim 2016, Hamilton, Canada, accepted, 2016.
[10] R. Moffat, Describing the Uncertainties in Experimental Results, Experimental Thermal and Fluid Science 1 (1988) 3–17.